ARTICLES

Selective Modification of the Channel Entrances of Zeolite L with Triethoxysilylated Coumarin

Takayuki Ban, Dominik Brühwiler, and Gion Calzaferri*

Department of Chemistry and Biochemistry, University of Bern, Freiestrasse 3, CH-3000 Bern 9, Switzerland

Received: April 5, 2004; In Final Form: August 6, 2004

The insertion of a triethoxysilylated coumarin dye into the channels of zeolite L from CH_2Cl_2 was examined. Fluorescence from the dye was observed only at the base planes of the cylindrical zeolite L crystals, indicating selective modification of the channel entrances. Leaching of the dye was observed when the material was dispersed in ethanol immediately after the insertion, suggesting reversibility of adsorption. A stable material was obtained after refluxing in toluene. This procedure led to the formation of covalent siloxane bonds between the triethoxysilyl group and silanol groups at the entrances of the zeolite channels. Hence, selective modification of the channel entrances is achieved via consecutive insertion and covalent bond formation processes. An appropriate choice of solvent for the insertion step is crucial. When zeolite L crystals containing pyronine were modified with the triethoxysilylated coumarin and irradiated at 335 nm, energy transfer from the coumarin to pyronine was observed.

Introduction

Zeolites are crystalline aluminosilicates with molecular-size cavities or channels. They have been successfully employed for obtaining highly organized arrangements of a large variety of guest species.[1] When zeolites with hexagonal framework accommodate a dye as a guest, the following properties are expected:[2] (1) Zeolites are transparent from ultraviolet to the near-IR and thus do not interfere with light absorption and emission of the dye. (2) Confinement of a dye in a cavity or channel can prevent aggregation, resulting in stabilization of the respective monomer. (3) The periodic arrangement of channels leads to orientation of the accommodated dyes. When dye molecules inside the channels are used for photonic energy migration and transfer between themselves via dipole−dipole interaction, the third feature is important, because the efficiency of radiationless electronic excitation energy migration and transfer is largely influenced by the relative orientation of the dye molecules, as well as by their intermolecular distances and photophysical properties. Zeolite L, which has a typical composition of $K_9Al_9Si_{27}O_{72}\cdot xH_2O$ and one-dimensional channels with an aperture size of 0.71 nm, has been employed as host for a large variety of dye molecules, and energy migration and transfer have been observed in dye−zeolite L composites, thereby qualifying them as efficient photonic antennae.[2−4]

Communication between materials by means of photonic energy attracts considerable interest.[5] When, for example, a composite of a dye−zeolite guest−host material and a semiconductor is envisaged to enable energy transfer between the dyes and the semiconductor, it is necessary to develop the interface between them so that photonic energy is transferred efficiently. Transfer of photonic energy from the dye in the channels directly to the semiconductor seems problematic. A promising approach for the modification of the interface is to plug the entrances of the zeolite channels with dye molecules (stopcock dye molecules) and then establish contact between these dyes and the semiconductor surface.[4] Photonic energy harvested by the dye molecules inside the channels would then be transferred to the stopcock dye and subsequently from the stopcock dye to the semiconductor. Several types of stopcock molecules have been developed for zeolite L.[4,6,7] An example is a molecule containing head, spacer, and label moieties, with the head being too large to enter the zeolite L channel.[4,6] Head and label moieties are composed of fluorescent dyes and separated by a flexible spacer. Insertion of the spacer and label moieties into the channel entrances of a dye−zeolite L guest−host material allows transfer of photonic energy from a dye inside the channel to the stopcock head or label moiety. An appropriate choice of dyes also enables reverse energy transfer. A drawback of this type of stopcock molecule is that there is no covalent bond between the stopcock and the zeolite; that is, leaching may occur. Recently, a stopcock consisting of a large dye molecule with a dimethylethoxysilyl group $-Si(CH_3)_2(OC_2H_5)$ was reported.[7] While the dye moiety is too large to enter the zeolite L channel, the ethoxysilyl group can react with a silanol group at the channel entrance resulting in a covalent bond. When the dye−zeolite L guest−host material modified with this stopcock molecule was spread onto a silicon semiconductor, energy transfer from the dye−zeolite L guest−host material to the semiconductor via the stopcock was observed.[7] As a further improvement, one can envisage a stopcock molecule capable of forming covalent bonds with both the entrance of the zeolite channels and the semiconductor surface.

Here, we suggest a coumarin dye modified with a trialkoxysilyl group. Scheme 1 illustrates the general concept of the channel entrance modification with this coumarin derivative.

* Corresponding author. Telephone: +41 31 631 42 36. Fax: +41 31 631 39 94. E-mail: gion.calzaferri@iac.unibe.ch.

10.1021/jp048516i CCC: $27.50
Published on Web 09/16/2004

SCHEME 1: Selective Modification of Zeolite L Channel Entrances with Triethoxysilylated Coumarin

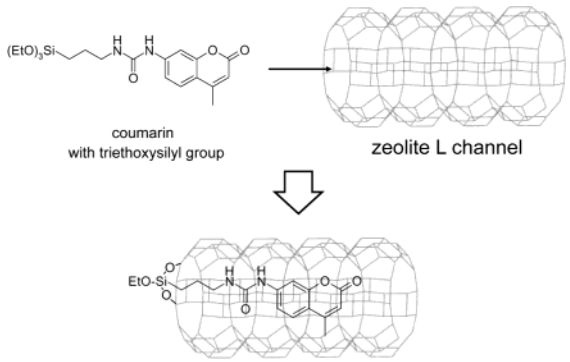

The coumarin moiety is small enough to enter the zeolite L channel, thereby orienting the stopcock molecule. The silane moiety of the stopcock consists of three alkoxy groups, that is, three reactive centers, which can be used for the formation of siloxane bonds with the zeolite channels and a semiconductor surface via a condensation reaction. Grafting of silane coupling agents having a trialkoxysilyl or trichlorosilyl group to zeolites[8,9] and mesoporous materials[10] has been investigated extensively. Yoon et al. have investigated the modification of zeolite crystal surfaces with trialkoxysilyl agents to obtain defined arrangements of zeolite crystals on a substrate.[8] In their study, the entire external surface of the zeolite crystals was modified and the functionality of the silane coupling agent is pointing outward. It is challenging to modify selectively the zeolite channel entrances with a dye moiety pointing inward as shown in Scheme 1. We demonstrate for the first time that zeolite channel entrances can be modified selectively in this manner, and we describe energy transfer from the stopcock molecule to a dye inside the channels.

Experimental Section

Synthesis of Zeolite L. Zeolite L crystals of different size were prepared (0.2, 0.8, and 5.2 μm average length). The synthesis of the smaller crystals is described elsewhere.[3] Zeolite L crystals with a length of 5.2 μm (see Figure 1) were synthesized by hydrothermally treating a gel with the composition of $2.2K_2O$:$1.0Al_2O_3$:$9.0SiO_2$:$161.6H_2O$ at 175 °C for 72 h without agitation. The details of the synthesis are as follows: Metallic aluminum powder was dissolved in a KOH aqueous solution in N_2 atmosphere under cooling with ice. The obtained potassium aluminate solution was filtered for removal of $Fe(OH)_3$ colloid impurities and then added to a colloidal silica solution (Ludox HS-40), resulting in an opaque sol. The sol

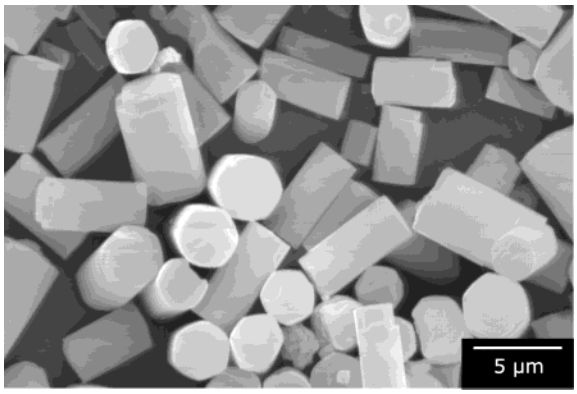

Figure 1. SEM image of zeolite L crystals (5.2 μm average length).

SCHEME 2: Synthesis of Triethoxysilylated Coumarin (TSPCU) and Structure of Pyronine (Py^+)

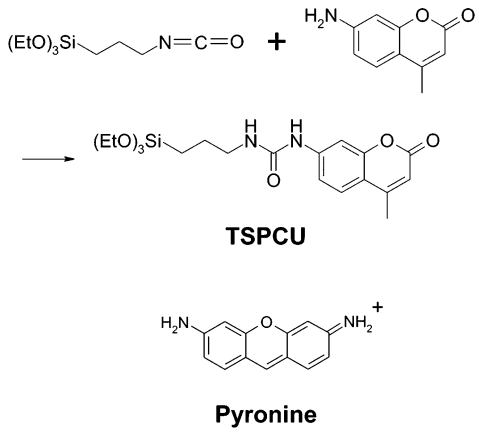

was stirred for 2 min at room temperature, transferred to a Teflon autoclave, and then treated hydrothermally under the above-mentioned conditions. The zeolite was recovered by centrifugation and washed with abundant hot water by repeating the centrifugation until the pH of the supernatant became lower than 8. For ion exchange, the zeolite was suspended in a KNO_3 aqueous solution and stirred at 50 °C for 5 h. The ion-exchanged zeolite was recovered by centrifugation and washed with abundant water by repeating the centrifugation until the pH of the supernatant became higher than 6.5.

Synthesis of Triethoxysilylated Coumarin. Triethoxysilylated coumarin (*N*-(3-triethoxysilylpropyl)-*N*′-{7-(4-methylcoumarin)} ureido; hereafter referred to as TSPCU) was synthesized by reaction of 7-amino-4-methylcoumarin (AMC, Aldrich 98%) with (3-isocyanatopropyl)triethoxysilane (IPTES, Aldrich 95+%) as shown in Scheme 2. The starting materials were used as received. First, 150 mg (0.86 mmol) of AMC was dissolved in 20 mL of dry THF. After 30 min of stirring, 4.25 mL (17.2 mmol) of IPTES was added, and the mixture was refluxed for 45 h. After the mixture was cooled to room temperature, the solvent was removed by evaporation. The precipitated powder was dissolved in 10 mL of dry CH_2Cl_2, and a very small amount of precipitate was removed by filtration through a cotton-packed pipe. Next, 20 mL of hexane was poured gently into the CH_2Cl_2 solution to precipitate the product. After the mixture was allowed to sit for 2 days, the product was recovered with suction filtration and washed with abundant hexane. This precipitation/purification scheme was repeated twice for optimal purity. Finally, 157 mg of a white powder (yield 43%, mp 200 °C) was obtained. ^{1}H NMR ($CDCl_3$): δ (ppm) 0.70 (t, 2H, $SiCH_2$), 1.23 (t, 9H, CH_3 in OEt), 1.70 (quin, 2H, middle CH_2 in propylene), 2.44 (s, 3H, arom$-CH_3$), 3.30 (quar, 2H, N$-CH_2$), 3.83 (quar, 6H, OCH_2), 5.62 (t, 1H, NH), 6.14 (s, 1H, arom$-$H), 7.51 (s, 1H, arom$-$H), 7.53 (d, 1H, arom$-$H), 8.07 (d, 1H, arom$-$H), 8.09 (s, 1H, arom$-$NH$-$). UV$-$vis spectroscopy (in ethanol): $\lambda_{max} = 333$ nm, $\epsilon = 2.2 \times 10^4$ M^{-1} cm^{-1}. Fluorescence spectroscopy (in ethanol): $\lambda_{max}^{ex} = 334$ nm, $\lambda_{max}^{em} = 401$ nm.

Selective Modification of the Zeolite L Channel Entrances with TSPCU. Selective modification as shown in Scheme 1 was conducted by dispersing zeolite L in a CH_2Cl_2 solution of TSPCU. In a typical experiment, 200 mg of zeolite L (5.2 μm length) was dehydrated by heating at 400 °C for 2 h in a vacuum, and then was suspended in 30 mL of a 0.8 μM CH_2Cl_2 solution of TSPCU. The suspension was sonicated for 10 min and then stirred at room temperature for 20 h. The zeolite was recovered by centrifugation, dried in a N_2 stream, and added

to 15 mL of dry toluene. The toluene suspension was refluxed for 2 h. The zeolite was recovered by centrifugation and dried in a N_2 stream. The added number of TSPCU molecules was set to twice the number of zeolite L channels for insertion of the stopcock molecules into both ends of the channels. The number of adsorbed TSPCU molecules was estimated from UV−vis absorption spectra (Perkin-Elmer, Lambda 900) of the starting solution used for the adsorption and the supernatant after the adsorption. The adsorption site of TSPCU was examined using a fluorescence microscope (Olympus BX 60 microscope equipped with a Kappa CF 20 DCX air-cooled CCD camera).

Energy Transfer from TSPCU Molecules at the Zeolite Channel Entrances to Pyronine Inside the Channels. Here, 0.2 μm long zeolite L crystals were used. Pyronine (Py^+, see Scheme 2) was inserted into the zeolite channels by ion exchange with potassium ions. After the zeolite was dispersed in an aqueous solution of pyronine acetate salt, the resulting suspension was sonicated for 10 min at room temperature and then refluxed for 18 h. The Py^+-loaded zeolite was collected by centrifugation, washed with a non-ionic surfactant (Genapol X-080, Fluka), and then rinsed with abundant water. The loading ratio of Py^+ was estimated from the concentrations of the starting solution and the supernatant of the suspension after the insertion process. Three samples with loading ratios of 0.130, 0.095, and 0.044 were prepared. The loading ratio is defined as the number of molecules per site. In the case of Py^+, a site consists of two unit cells of zeolite L; for details, see ref 2a. TSPCU was inserted into a Py^+−zeolite L sample by the method mentioned above, except for the dehydration step. To inhibit thermal decomposition of the included Py^+, dehydration was carried out via heating at 140 °C for 2 h in a vacuum. The added number of TSPCU molecules was set to twice the number of zeolite L channels. The energy transfer was evaluated by measuring fluorescence spectra (Perkin-Elmer, LS 50-B) of TSPCU−Py^+−zeolite L crystals spread onto quartz glass. Fluorescence and excitation spectra of TSPCU and Py^+ in zeolite L are shown in Figure 2.

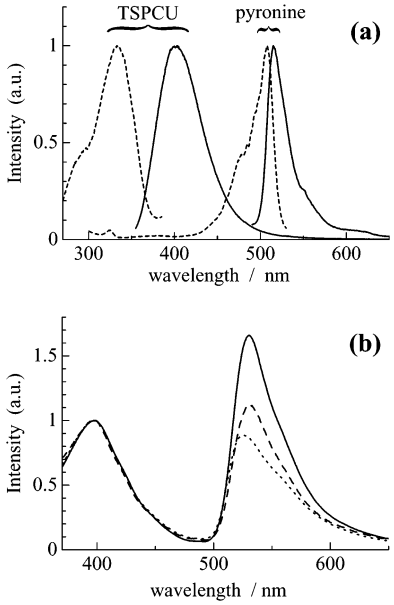

Figure 2. (a) Excitation (broken lines) and emission (solid lines) spectra of TSPCU−zeolite L and Py^+−zeolite L. The spectra were scaled to the same height. Excitation and emission spectra of TSPCU−zeolite L were measured at an emission wavelength of 410 nm and an excitation wavelength of 330 nm, respectively. Excitation and emission spectra of Py^+−zeolite L were measured at an emission wavelength of 560 nm and an excitation wavelength of 460 nm, respectively. (b) Emission spectra of TSPCU−Py^+−zeolite L with Py^+ loading ratios of 0.130 (solid line), 0.095 (broken line), and 0.044 (dotted line) upon excitation at 335 nm.

Results and Discussion

Synthesis of TSPCU. TSPCU was synthesized by the reaction shown in Scheme 2. It is well known that isocyanate groups can react easily with a functionality having a reactive proton, such as amino, hydroxy, and mercapto groups.[11] The reaction of isocyanate with amino groups results in the formation of a urea bridge −NHCONH−. However, the reaction of the amino group in AMC proceeded very little, even when 2 equiv of IPTES was added. As outlined in the Experimental Section, 20 equiv of IPTES was finally used. The excessive addition of IPTES may bring about two problems: contamination of the product with IPTES and reaction of the substituted urea bridge with IPTES, that is, formation of a biuret linkage. IR, DSC, and ^{1}H NMR measurements of the product confirmed that neither contamination nor formation of a biuret linkage was a problem. IR spectra did not exhibit isocyanate absorption bands around 2273 and 1718 cm^{-1}. The DSC curve showed a very sharp endothermic peak at 200 °C (melting) with a peak width at half-height of about 1 °C, indicating a product of high purity. The ^{1}H NMR spectrum of the product confirmed that the target compound TSPCU was obtained with high purity, although a very weak peak of an impurity was observed at 1.62 ppm. The contamination of the product with IPTES is avoided by washing thoroughly with hexane, taking advantage of the fact that IPTES is soluble in hexane while TSPCU is not. The further reaction of the urea bridge with IPTES is expected to be slow, because the amide group has only one reactive proton and has reduced nucleophility. The reason the amino group in AMC features a relatively low reactivity remains unclear, although we can speculate that steric hindrance or an unfavorable charge density distribution might play a role.

The UV−vis absorption spectrum of an ethanol solution of TSPCU showed $\lambda_{max} = 333$ nm and $\epsilon = 2.2 \times 10^4$ M^{-1} cm^{-1}, whereas λ_{max} and ϵ of an ethanol solution of the precursor coumarin AMC were 354 nm and 1.8×10^4 M^{-1} cm^{-1}, respectively. The emission spectrum of an ethanol solution of TSPCU featured $\lambda_{max} = 401$ nm (excitation at 330 nm), whereas that of AMC exhibited $\lambda_{max} = 428$ nm (excitation at 350 nm). The reaction of AMC with IPTES leads to a blue shift in absorption and emission of the coumarin, which can be attributed to a change of electron-donating ability in the 7-site substituent of the coumarin upon replacing the amino group with a urea bridge.

Insertion of TSPCU into the Zeolite L Channel Entrances. Selective modification of the zeolite L channel entrances with TSPCU, as shown in Scheme 1, was conducted in solution. Among the investigated solvents, TSPCU was found to be soluble in solvents more polar than chloroform, that is, a solvent with a specific dielectric constant higher than 4.8. Solutions of CH_2Cl_2, THF, and mixtures thereof were tested for the insertion of TSPCU. A dehydrated zeolite L sample was dispersed in a CH_2Cl_2 solution of TSPCU in which the number of TSPCU molecules was equal to that of zeolite L channel entrances (24 μM in this case). The absorption spectrum of the supernatant of this CH_2Cl_2 suspension showed that all of the added TSPCU molecules were adsorbed onto the zeolite crystals, while only 25% were adsorbed from a THF solution. When the zeolite crystals collected from the CH_2Cl_2 suspension were dispersed in ethanol, more than 60% of the adsorbed TSPCU molecules

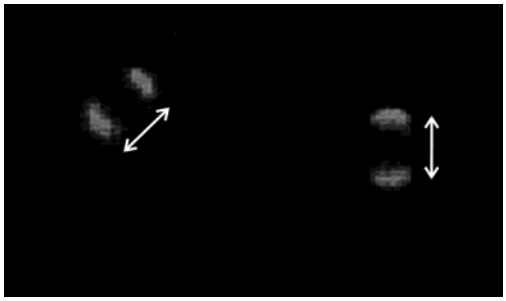

Figure 3. Gray-scale fluorescence microscopy image of two zeolite L crystals modified with TSPCU. The image was observed while irradiating with UV light in the wavelength range between 330 and 385 nm. An emission filter transmitting light of wavelength longer than 420 nm was used. The length of the crystals is approximately 5 μm and is indicated by arrows.

were leached out of the zeolite. However, TSPCU leaching was not observed after refluxing the material in toluene. These results indicate that TSPCU prefers adsorbing onto zeolite L to dissolving in CH_2Cl_2 and that this solvent results in a much stronger tendency toward adsorption of TSPCU onto the zeolite crystals than THF or ethanol. Furthermore, it can be concluded that the adsorption of TSPCU from CH_2Cl_2 solution is reversible and therefore not due to siloxane bond formation between surface silanols of the zeolite and ethoxysilyl in TSPCU. Siloxane bonds are only formed upon refluxing the TSPCU−zeolite crystals in toluene.

The adsorption site of TSPCU was examined by means of fluorescence microscopy. A CH_2Cl_2 solution with a TSPCU concentration of 0.8 μM was used for the insertion. Again, the number of TSPCU molecules was set equal to the number of zeolite L channel entrances. Crystals of 5.2 μm average length were used for these experiments. Figure 3 shows a fluorescence microscopy image of the prepared sample. The fluorescence spectrum of a TSPCU−zeolite L composite is shown in Figure 2a. The excitation spectrum exhibited λ_{max} at 333 nm (emission at 410 nm), whereas the emission spectrum exhibited λ_{max} at 400 nm (excitation at 330 nm). The fluorescence spectra of TSPCU−zeolite L are similar to those of an ethanol solution of TSPCU. The adsorption of TSPCU onto zeolite L apparently does not influence the TSPCU luminescence. In the fluorescence microscopy image, twins of blue light assigned to the fluorescence of TSPCU were observed upon UV irradiation (330−385 nm). These twins are located at the edges of the crystals, that is, the base planes, indicating that TSPCU is adsorbed preferentially at the channel entrances. Achievement of this selective modification is attributed to the separation of the insertion and covalent bond formation processes and to an appropriate choice of solvent used for the insertion (see Figure 4).

Energy Transfer from TSPCU to Py^+ Inside the Channels. Energy transfer from TSPCU molecules at the channel entrances to Py^+ inside the channels was examined using TSPCU−Py^+−zeolite L crystals with an average length of 0.2 μm. Figure 2a shows excitation and emission spectra of TSPCU and Py^+ in zeolite L. The emission spectrum of TSPCU partially overlaps the excitation spectrum of Py^+, indicating that energy transfer from TSPCU to Py^+ is possible. Figure 2b shows emission spectra of TSPCU−Py^+−zeolite L upon excitation at 335 nm, which corresponds to a specific excitation of TSPCU. Fluorescence from TSPCU and Py^+ was observed around 400 and 530 nm, respectively. For comparison of the spectra, the maximum intensity of the emission of TSPCU was normalized. The relative intensity of fluorescence from Py^+ increased with increasing

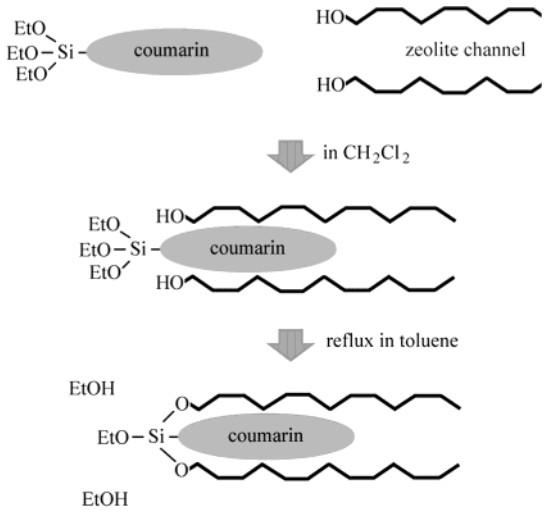

Figure 4. Separation of the insertion and covalent bond formation processes in the modification of zeolite L channel entrances with triethoxysilylated coumarin.

loading. Obviously, energy transfer from TSPCU to Py^+ contributes to this intensity change. The probability of radiationless electronic excitation energy transfer is inversely proportional to the sixth power of distance between the dyes.[4] Increasing the acceptor loading leads to a decrease in the distance to TSPCU at the entrances of the channels and therefore to an increase in the probability of energy transfer. Despite the relatively small overlap between the emission spectrum of TSPCU and the excitation spectrum of Py^+, substantial energy transfer could be observed. It is expected that a more appropriate combination of donor and acceptor dyes would lead to an increase in energy-transfer efficiency.

Conclusions

Insertion of a triethoxysilylated coumarin into zeolite L from a CH_2Cl_2 solution was successful. The insertion process leads to a selective modification of the zeolite L channel entrances through the formation of covalent siloxane bonds between dye and zeolite upon refluxing in toluene. High selectivity is achieved by separation of the insertion and covalent bond formation processes. When zeolite L with Py^+ inside the channels was modified with the triethoxysilylated coumarin, energy transfer from the coumarin to Py^+ was observed. This selective modification, which can be applied to dyes other than coumarin, is expected to provide a useful interface for efficiently mediating photonic energy transfer between dye−zeolite guest−host materials and a semiconductor. In other applications, a novel anisotropic property might emerge from the selective functionalization of zeolite channel entrances. Furthermore, the ability to effectively close the channel entrances of zeolites is highly desirable for systems in which the guest−zeolite interactions are weak. Covalently bound stopcock molecules can prevent guest molecules from leaving the channels while also restricting the diffusion of external species into the channels.

Acknowledgment. Financial support by the Swiss National Science Foundation (Project NFP 47, 4047-057481) is acknowledged. We also thank the Bundesamt für Bildung und Wissenschaft (BBW Switzerland) for financial support within the European Union Project "RTN Nanochannel". Dr. Takayuki Ban acknowledges support from a visiting research fellowship program by the Japanese Ministry of Education, Sports, Science, and Technology. We thank Dr. Marieke van Veen for performing IR measurements.

Note Added in Proof. This article was posted ASAP on 9/16/2004. In the last paragraph of the Experimental Section, the word anionic has been changed to non-ionic. The correct version was posted on 9/22/2004.

References and Notes

(1) (a) Ganschow, M.; Hellriegel, C.; Kneuper, E.; Wark, M.; Thiel, C.; Schulz-Ekloff, G.; Bräuchle, C.; Wöhrle, D. *Adv. Funct. Mater*. **2004**, *14*, 269−276. (b) Corma, A.; Garcia, H. *Eur. J. Inorg. Chem.* **2004**, 1143−1164. (c) Brühwiler, D.; Calzaferri, G. *Microporous Mesoporous Mater*. **2004**, *72*, 1−23.

(2) (a) Calzaferri, G.; Maas, H.; Pauchard, M.; Pfenniger, M.; Megelski, S.; Devaux, A. *Adv. Photochem.* **2002**, *27*, 1−50. (b) Gfeller, N.; Calzaferri, G. *J. Phys. Chem. B* **1997**, *101*, 1396−1408. (c) Gfeller, N.; Megelski, S.; Calzaferri, G. *J. Phys. Chem. B* **1998**, *102*, 2433−2436. (d) Gfeller, N.; Megelski, S.; Calzaferri, G. *J. Phys. Chem. B* **1999**, *103*, 1250−1257. (e) Pfenniger, M.; Calzaferri, G. *ChemPhysChem* **2000**, *1*, 211−217. (f) Calzaferri, G.; Pauchard, M.; Maas, H.; Huber, S.; Khatyr, A.; Schaafsma, T. *J. Mater. Chem.* **2002**, *12*, 1−13.

(3) Megelski, S.; Calzaferri, G. *Adv. Funct. Mater*. **2001**, *11*, 277−286.

(4) Calzaferri, G.; Huber, S.; Maas, H.; Minkowski, C. *Angew. Chem., Int. Ed.* **2003**, *42*, 3732−3758.

(5) Dexter, D. L. *J. Lumin.* **1979**, *18/19*, 779−784.

(6) (a) Maas, H.; Calzaferri, G. *Angew. Chem., Int. Ed.* **2002**, *41*, 2284−2288. (b) Khatyr, A.; Maas, H.; Calzaferri, G. *J. Org. Chem.* **2002**, *67*, 6705−6710.

(7) Huber, S.; Calzaferri, G. *ChemPhysChem* **2004**, *5*, 239−242.

(8) (a) Kulak, A.; Lee, Y.-J.; Park, Y. S.; Yoon, K. B. *Angew. Chem., Int. Ed.* **2000**, *39*, 950−953. (b) Choi, S. Y.; Lee, Y.-J.; Park, Y. S.; Ha, K.; Yoon, K. B. *J. Am. Chem. Soc.* **2000**, *122*, 5201−5209. (c) Ha, K.; Lee, Y.-J.; Lee, H. J.; Yoon, K. B. *Adv. Mater.* **2000**, *12*, 1114−1117. (d) Lee, G. S.; Lee, Y.-J.; Yoon, K. B. *J. Am. Chem. Soc.* **2001**, *123*, 9769−9779. (e) Park, J. S.; Lee, G. S.; Lee, Y.-J.; Park, Y. S.; Yoon, K. B. *J. Am. Chem. Soc.* **2002**, *124*, 13366−13367. (f) Park, J. S.; Lee, Y.-J.; Yoon, K. B. *J. Am. Chem. Soc.* **2004**, *126*, 1934−1935.

(9) (a) Sano, T.; Yamada, K.; Ejiri, S.; Hasegawa, M.; Kawakami, Y.; Yanagishita, H. *Stud. Surf. Sci. Catal.* **1997**, *105*, 2179−2186. (b) Kawai, T.; Tsutsumi, K. *Colloid Polym. Sci.* **1998**, *276*, 992−998. (c) Impens, N. R. E. N.; van der Voort, P.; Vansant, E. F. *Microporous Mesoporous Mater*. **1999**, *28*, 217−232.

(10) (a) Moller, K.; Bein, T. *Chem. Mater*. **1998**, *10*, 2950−2963. (b) Feng, X.; Fryxell, G. E.; Wang, L.-Q.; Kim, A. Y.; Liu, J.; Kemner, K. M. *Science* **1997**, *276*, 923−926. (c) Mercier, L.; Pinnavaia, T. J. *Adv. Mater.* **1997**, *9*, 500−503. (d) Liu, J.; Feng, X.; Fryxell, G. E.; Wang, L.-Q.; Kim, A. Y.; Gong, M. *Adv. Mater.* **1998**, *10*, 161−165. (e) Xu, W.; Luo, Q.; Wang, H.; Francesconi, L. C.; Stark, R. E.; Akins, D. L. *J. Phys. Chem. B* **2003**, *107*, 497−501. (f) Mal, N. K.; Fujiwara, M.; Tanaka, Y. *Nature* **2003**, *421*, 350−353.

(11) *Advances in Urethane Science and Technology*; Klempner, D., Frisch, K. C., Eds.; Chem Tec Publishing: Toronto, 2001.